

Measurement of Interstellar Polarization and Estimation of Galactic Extinction for the Direction of X-ray Black Hole Binary V404 Cygni

Ryosuke ITOH^{1,1a}, Yasuyuki T. TANAKA², Koji S. KAWABATA², Makoto UEMURA², Makoto WATANABE^{3,3a}, Yasushi FUKAZAWA¹, Yuka KANDA¹, Hiroshi AKITAYA², Yuki MORITANI^{2,4}, Tatsuya NAKAOKA¹, Miho KAWABATA¹, Kensei SHIKI¹, Michitoshi YOSHIDA², Yumiko OASA⁵ and Jun TAKAHASHI⁶

¹Department of Physical Science, Hiroshima University, Higashi-Hiroshima, Hiroshima 739-8526, Japan

^{1a}School of Science, Tokyo Institute of Technology, 2-12-1 Ohokayama, Meguro, Tokyo 152-8551, Japan; : itoh@hp.phys.titech.ac.jp

²Hiroshima Astrophysical Science Center, Hiroshima University, Higashi-Hiroshima, Hiroshima 739-8526, Japan

³Department of CosmoSciences, Graduate School of Science, Hokkaido University, Kita 8, Nishi 10, Kita-ku, Sapporo, Hokkaido 060-0810, Japan

^{3a}Department of Applied Physics, Faculty of Science, Okayama University of Science, 1-1 Ridai-cho, Okayama, Okayama 700-0005, Japan

⁴Kavli Institute for the Physics and Mathematics of the Universe (WPI), The University of Tokyo Institutes for Advanced Study, The University of Tokyo, Kashiwa, Chiba 277-8583, Japan

⁵Faculty of Education, Saitama University, 255 Shimo-Okubo, Sakura, Saitama, Saitama 338-8570, Japan

⁶Nishi-Harima Astronomical Observatory, Center for Astronomy, University of Hyogo, 407-2, Nishigaichi, Sayo-cho, Sayo, Hyogo 679-5313, Japan

Received ; Accepted

Abstract

V404 Cygni is a well-known black hole binary candidate thought to have relativistic jets. It showed extreme outbursts on June 2015, characterized by a large amplitude and short time variation of flux in the radio, optical, and X-ray bands. Not only disk emission, but also synchrotron radiation from the relativistic jets were suggested by radio observations. However, it is difficult to measure the accurate spectral shape in the optical/near infrared band because there are uncertainties of interstellar extinction.

To estimate the extinction value for V404 Cygni, we performed photopolarimetric and spectroscopic observations of V404 Cygni and nearby field stars. Here, we estimate the Galactic extinction using interstellar polarization based on the observation that the origin of the optical polarization is the interstellar medium, and investigate the properties of interstellar polarization around V404 Cygni. We found a good correlation between the color excess and polarization degree in the field stars. We also confirmed that the wavelength dependence of the polarization degree in the highly polarized field stars was similar to that of V404 Cygni. Using the highly polarized field stars, we estimated the color excess and the extinction, $E(B - V) = 1.2 \pm 0.2$

and $3.0 < A(V) < 3.6$, respectively. A tendency for a bluer peak of polarization ($\lambda_{\max} < 5500 \text{ \AA}$) was commonly seen in the highly polarized field stars, suggesting that the dust grains toward this region are generally smaller than the Galactic average. The corrected spectral energy distribution of V404 Cygni in the near infrared (NIR) and optical bands in our results indicated a spectral break between $2.5 \times 10^{14} \text{ Hz}$ and $3.7 \times 10^{14} \text{ Hz}$, which might be originated in the synchrotron self absorption.

1 Introduction

The radiation from microquasars often suffers from Galactic extinction and polarization by the interstellar medium, making it difficult to determine the nature of these objects. Polarization in the near infrared (NIR) is one sign of synchrotron radiation in several microquasars (Shahbaz et al. 2008) and is an important measurement used to investigate the environment of the jet and the origin of variability in the microquasars. However, the radiation is often contaminated by interstellar polarization (ISP). In addition, the Galactic extinction makes it difficult to measure the intrinsic spectral shape of microquasars in the optical and NIR bands. It is important to investigate the actual properties of the interstellar medium to determine the precise emission model for microquasars.

V404 Cygni (a.k.a, GS 2023+338) is a well-known X-ray black hole binary with $12 \pm 3 M_{\odot}$ masses (Shahbaz et al. 1994) at a distance of 2.4 kpc (Miller-Jones et al. 2009). It showed extreme outbursts in June 2015, with large amplitude variability and a time scale of seconds to hours in the radio, optical, and X-ray bands (e.g., Kimura et al. 2016). In contrast to the large variation in total flux, there were very small variability of polarization in the optical or NIR bands. Tanaka et al. (2016) reported no significant variability of polarization in the optical and NIR bands, while Shahbaz et al. (2016) and Lipunov et al. (2016) detected very small polarization variation in limited time intervals which were not covered by Tanaka et al. (2016). This implies that disk or optically-thick synchrotron emission (or both) dominated in the NIR regime.

To obtain an accurate spectrum in the optical/NIR band, careful estimation of the Galactic extinction is needed. Casares et al. (1993) performed high-resolution spectroscopic observation of V404 Cygni in 1991, and they estimated the spectral type of comparison star as K0(-1) III-IV. From this result, they determined the Galactic absorption of $A(V) = 4.0$. Shahbaz et al. (1994), however, suggested the Galactic absorption of $A(V) < 3.3$ by NIR-band photometry of V404 Cygni and a tripped giant model.

Here, we estimated the color excess of V404 Cygni by measuring interstellar polarization and color excess for the surrounding field stars. The distinctive feature of our method is that we do not require any assumption of intrinsic luminosity and color of comparison stars in microquasars. In this paragraph, we introduce the basic principles of our method. The relation

between color excess originating in the Galactic extinction and ISP has been well studied (e.g., Fosalba et al. 2002). In general, the polarization degree (PD) of ISP increases with color excess. It is also known that the wavelength dependence of ISP in ultraviolet to NIR bands is well described by the Serkowski-law (Serkowski et al. 1975, details also described in Section 3.1). A wavelength at peak PD is related to the ratio of extinction and color excess, defined as $R_V = A(V)/E(B - V)$, where $A(V)$ is extinction in the V-band and $E(B - V)$ is the color excess for $B - V$ color. To estimate the contribution of interstellar extinction and polarization for V404 Cygni, we performed optical and NIR polarimetric observations of V404 Cygni and nearby stars. First, we measured the color excess and ISP for the field stars around V404 Cygni and clarified the relations between these parameters. Then, we estimated the color excess of V404 Cygni from its PD value. From a measurement of the wavelength dependence of V404 Cygni, we estimated the R_V value with the Serkowski-law. Using these two parameters, $E(B - V)$ and R_V , we estimated the Galactic extinction for V404 Cygni.

2 Observation

2.1 Photopolarimetric observation

We performed V -, R_C -, I_C -, J -, H - and K_s -band photopolarimetric observation of V404 Cygni and field stars on 22 June 2015 using the Hiroshima Optical and Near Infrared camera (HONIR, Akitaya et al. 2014) installed on the 1.5 m Kanata telescope, located at Higashi-Hiroshima Observatory in Japan. We also performed long-term photopolarimetric monitoring of V404 Cygni in the R_C -band from 17 June 2015 to 27 September 2015 with a multi-spectral imager (MSI, Watanabe et al. 2012) installed on the 1.6 m Pirka telescope at Nayoro Observatory of Hokkaido University in Japan. Each observation consisted of a sequence of exposures at four position angles of the achromatic half-wave plates, 0.0, 22.5, 45.0, and 67.5 degree. The field of view of HONIR for polarimetric observation consisted of five rectangles ($0.8 \text{ arcmin} \times 10 \text{ arcmin}$) separated on the side by 0.8 arcmin. We confirmed that instrumental polarization of HONIR was less than 0.1% in the optical band and 0.2% in the NIR-band by observation of unpolarized standard stars (HD212311 and G191B2B, Schmidt et al. 1992). We also corrected the instrumental depolarization by measurement of an artificially 100% polarized star, with a wire-grid polarizer for each

band. The origins of the polarization angle were calibrated with the strong polarized stars, HD150193 and HD19820 (Whittet et al. 1992). Each measured PD and PA after all calibrations were consistent with catalog values of strong polarized stars, with uncertainties of $\Delta PD \sim 0.1\%$ and $\Delta PA \sim 2$ degrees, respectively.

We used archival data of *Swift* observation for the field stars around V404 Cygni on MJD54947. We used the *B* and *V*-band photometric data taken by the UV and Optical Telescope (UVOT). UVOT data were reduced following the standard procedure for CCD photometry. Counts were extracted from an aperture of 5 arcsec radius for all filters and annulus background regions were sampled 27 arcsec away from object stars, and then converted to a flux using the standard zero points (Poole et al. 2008).

2.2 Spectroscopic observation

To determine the spectral type of the field stars, we performed low-resolution spectroscopic observations of field stars with Hiroshima One-shot Wide-field Polarimeter (HOWPol, $0.41\text{--}0.94 \mu\text{m}$, $R = \lambda/\Delta\lambda \sim 400$, Kawabata et al. 2008) on the Kanata Telescope from 24 to 30 July 2015. To investigate the relation between PD and color excess, we selected four bright field stars, with weak to strong polarization ($0.1\% < PD < 6\%$ in the *R_C*-band), for optical spectroscopic observation. In addition, we intensively performed spectroscopic observation of all field stars which have strong polarization ($PD > 7\%$ in the *R_C*-band) in order to securely compare with V404 Cyg. In total we obtained seven spectroscopic observation of field stars with weak to strong polarization ($0.1\% < PD < 8\%$ in the *R_C*-band). Table 1 shows the positions of field stars. The typical total exposure time for each star was about 30 minutes. The calibration of wavelength was performed with atmospheric emission lines for each frame. The flux was calibrated using observations of a spectrophotometric standard star (HR7596) obtained on the same nights.

Table 1. List of Field star around V404 Cygni

Name ¹	Coordinate ²
FS1	20:24:19.5 +33:52:42.3
FS2	20:24:11.9 +33:49:11.5
FS3	20:23:56.0 +33:53:28.7
FS4	20:23:57.1 +33:52:39.0
FS5	20:23:56.4 +33:48:16.9
FS6	20:23:49.2 +33:50:08.2
FS7	20:23:49.7 +33:48:23.5
V404 Cygni	20:24:03.8 +33:52:02.2

1: Name in this paper. Their positions are shown in Fig. 2, 2:Right ascension and declination (J2000)

3 Results

3.1 Interstellar polarization

Tanaka et al. (2016) reported no temporal variability of optical linear polarization for V404 Cygni, although it showed extreme flares. Figure 1 shows *R_C*-band light curve and temporal measurement of polarization for V404 Cygni from June to September 2015. In order to investigate the variability of PD, we adopted the constant fitting for the temporal variability of PD. Average value of PD is $7.8 \pm 0.1\%$ with χ^2_ν value of $\chi^2_\nu/\text{d.o.f} = 9.40/16$ which corresponds to the p-value of 0.89. It implied that there are no significant variability of PD between the active and quiescent states.

Figure 2 shows the multi-band polarization map around V404 Cygni. From this figure, the polarization angles (PAs) of field stars tends to an average of 7 degree and a standard deviation of 15 degree and V404 Cygni also shows a similar trend in the *R_C*-band. These trends of PA were also observed in the other band. Some field stars showed a small PD ($0\% < PD < 8\%$), but their PA tended to align with the whole trend. These results indicate that V404 Cygni has interstellar polarization due to the interstellar medium between the Earth and sources. Figure 3 shows the wavelength dependence of polarization for V404 Cygni and field stars between the optical *V*-band and NIR *K_s*-band. For comparison, the wavelength dependence of polarization for field stars that have a high-polarization degree (FS1, FS2, FS4, and FS7) are also shown in Figure 3. PD and PA values for V404 Cygni are also listed in Table 2. The maximum PD of V404 Cygni is $PD = 8.9 \pm 0.1\%$ in the *V*-band, and PD decreased with wavelength, showing no clear peak down to 5500 Å. This implies that the peak wavelength is located at shorter wavelengths ($< 5500\text{Å}$). On the other hand, the PA was constant for all wavelengths, with an average value of $PA = 8 \pm 2$ degrees. V404 Cygni and all of the field stars with a high PD showed similar trends. This implies that the dust grains aligned by the interstellar magnetic field toward this region are generally smaller than the Galactic average (e.g., Whittet 2003; Kawabata et al. 2014). We adopted the Serkowski+Wilking law (Serkowski et al. 1975) for the wavelength dependence of PD for V404 Cygni, as described below, $PD_{\text{Ser}} = p_{\text{max}} \times \exp\left(-\left(1.66 \times 10^{-4} \lambda_{\text{max}} + 0.01\right) \ln^2 \frac{\lambda}{\lambda_{\text{max}}}\right)$. Fitting shows $\lambda_{\text{max}} = 3000 \pm 1000 [\text{Å}]$ and $p_{\text{max}} = 10 \pm 2\%$. The χ^2_ν value is $\chi^2_\nu/\text{d.o.f} = 30.13/4$ for the fitting. The results of fitting implied a peak wavelength at $\lambda_{\text{max}} = 3000 [\text{Å}]$, but the original data did not show a clear peak. Therefore, we used an upper limit of $\lambda_{\text{max}} < 5500 [\text{Å}]$ as the peak wavelength for calculation of extinction.

For comparison, we also adopted a simple power-law fitting for the PD dependence of wavelength, which are related to an analog of the "IR polarization excess" found in the Galactic ISP at longer wavelengths (e.g., Nagata 1990), described as

$$PD_{PL} = P_0 \lambda^{-\beta}, \quad (1)$$

in Figure 3. The wavelength dependence of PD is well represented with $\beta = 1.2 \pm 0.1$ and $\chi^2_{\nu}/d.o.f = 110.96/4$. We note that the value of $\beta = 1.2$ obtained for the region of V404 Cygni is slightly shallow compared with the typical value of $\beta = 1.5 - 2.0$ for Galactic sources.

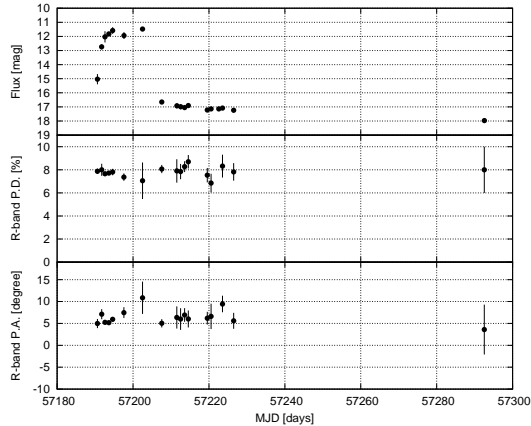


Fig. 1. Long-term light curve and temporal variability of R_C -band polarization of V404 Cygni. Top panel shows R_C -band light curve. 2nd panel shows temporal variability of polarization degree and bottom panel shows temporal variability of polarization angle.

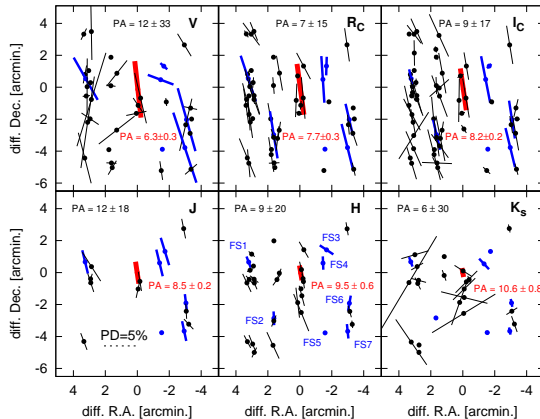


Fig. 2. Interstellar polarization map around V404 Cygni in the optical in the near infrared band. Length of bar shows polarization degree (scales are also shown in the left bottom panel) and direction of bar shows polarization angle on the celestial sphere. Red data and text indicates the data of polarization for V404 Cygni. Blue data indicate the data of field stars (FS1 to 7, also shown in center bottom panel). Black data point indicates the data of polarization for the other field stars in the field of view. Left top text shows average value of polarization angle of field stars (blue and black data points) for each band.

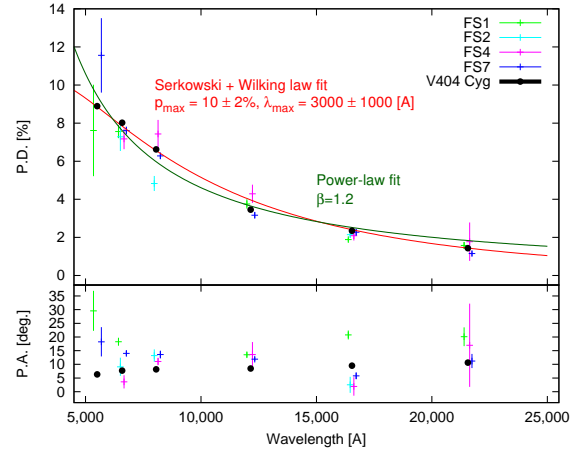


Fig. 3. Multi-band polarization of V404 Cygni and field stars which showed high polarization degree. Top panel shows the dependence for polarization degree with wavelength and bottom panel shows the dependence for polarization angle with wavelength. Red line indicates the results of Serkowski-law + Wilking-law fitting, and green line indicates the results of power-law fitting (details are described in text). Note that in order to be easily seen, we shifted the wavelength value for field stars.

Table 2. PD and PA value for V404 Cygni

Band	Wavelength [\AA]	PD [%]	PA [deg.]
V	5504	8.9 ± 0.1	6.3 ± 0.3
R_C	6587	8.0 ± 0.1	7.6 ± 0.3
I_C	8059	6.6 ± 0.1	8.1 ± 0.1
J	12149	3.5 ± 0.1	8.4 ± 0.1
H	16539	2.3 ± 0.1	9.5 ± 0.6
K_s	21555	1.4 ± 0.1	10.6 ± 0.7

3.2 Estimation of Color excess

Figure 4 shows the optical spectra of field stars FS1-7 obtained by HOWPOL. Comparing the patterns of dominant spectral features (e.g., H_{α} , Ca IR triplet, TiO bands) with the template spectral atlas of standard stars (Silva & Cornell 1992), we estimated the spectral type of FS1-7. For comparison, some template spectra of standard stars are also shown in Figure 4. Then, we measure the colour excess $E(R_C - I_C) = (R - I)_{\text{observed}} - (R - I)_{\text{intrinsic}}$, using $(R_C - I_C)_{\text{observed}}$ obtained from our observations and $(R_C - I_C)_{\text{intrinsic}}$ from well-studied field stars which have the same spectral type as the stars in FS1-7 (Wenger et al. 2000). The same methods were used for the derivation of $E(B - V)$ with UVOT data. The uncertainties of color excess depended on the classification of spectral type. Finally, we adopted the correction of extinction for the optical spectra based on the estimated color excess. The measurements are summarized in Table 3.

Figure 5 shows a scatter plot for PD, color ($R_C - I_C$), estimated color excess $E(R_C - I_C)$ and $E(B - V)$ for V404 Cygni

Table 3. Summary of properties for field stars

Name	Spectral type ¹	Flux [mag.] ²	P.D. [%] ³	$R_C - I_C^4$	$E(R_C - I_C)^5$	$E(B - V)^6$
FS1	K7 – M2	15.5	7.6 ± 0.3	1.77 ± 0.02	0.8 ± 0.2	1.0 ± 0.3
FS2	K0 – K4	16.2	7.5 ± 0.7	1.49 ± 0.02	1.0 ± 0.1	1.6 ± 0.5
FS3	A5 – A9	14.6	2.9 ± 0.2	0.67 ± 0.02	0.5 ± 0.1	0.8 ± 0.1
FS4	G8 – K4	16.1	7.3 ± 0.5	1.75 ± 0.02	1.3 ± 0.1	0.8 ± 0.6
FS5	F0 – F7	12.3	0.16 ± 0.05	0.31 ± 0.02	0.1 ± 0.1	0.2 ± 0.1
FS6	M0 – M5	13.6	5.1 ± 0.5	2.47 ± 0.02	1.6 ± 0.5	1.3 ± 0.1
FS7	K0 – K4	14.5	7.6 ± 0.2	1.60 ± 0.02	1.1 ± 0.1	1.5 ± 0.1

1: Estimated spectral type, 2: Observed magnitude in the R_C -band, 3: Observed optical polarization degree in the R_C -band, 4: Observed $R_C - I_C$ color, 5: Estimated color excess $E(R_C - I_C)$, 6: Estimated color excess $E(B - V)$.

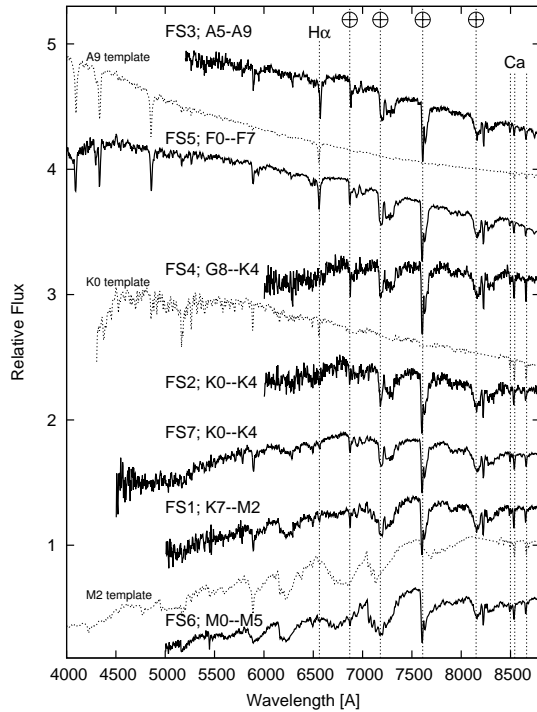


Fig. 4. The optical spectra of field stars obtained by HOWPol. Correction of extinction are performed by estimated color excess. Dashed lines show the spectrum template for standard stars (Wenger et al. 2000). The mark of \oplus indicate the telluric absorption lines. Summary of estimated spectral type and color excess are listed in Table 3.

and field stars. We also plotted all of the data points of field stars (not FS stars) in a scatter plot for color and polarization with black data points. From this figure, we can see that there is a general increase in PD with color and color excess.

The field stars FS1, FS2, FS4, and FS7 show similar properties of PD and color excess (see Table 3). From these results, we estimated the color excess of V404 Cygni. Using average value of color excess of the field stars FS1, FS2, FS4 and FS7, we estimated the color excess of $E(R_C - I_C) = 1.0 \pm 0.2$ and $E(B - V) = 1.2 \pm 0.3$ for the PD value of $PD = 8.0 \pm 0.1\%$ for V404 Cygni. These values are consistent with the value derived by spectroscopic observations of A comparison star for

V404 Cygni (Casares et al. 1993). We note that these color excess values are derived based on the PD value during the outburst.

4 Discussion

The aligned polarization angle and wavelength dependence of polarization implies that the polarization observed in V404 Cygni originated in the interstellar medium (This is also discussed in Tanaka et al. 2016). On the other hand, Shahbaz et al. (2016) reported that PD value in quiescent state is $PD = 7.41 \pm 0.32\%$ on 2016 May 26. This value is slightly low compared with the PD value in 2015 outburst and several short time variability of PD which probably originated in the jet during the 2015 outburst were also reported (e.g., Shahbaz et al. 2016; Lipunov et al. 2016). But variability of PD are relatively rare phenomenon during the outburst and its variability amplitude of PD is small ($\Delta PD \sim 1 - 2\%$). Therefore, in this paper, we assumed that most of polarization originated in ISP. In this section, we estimate the Galactic extinction and discuss the dust properties of V404 Cygni.

From optical spectroscopic observations, we identified the spectral type and determined the color excess of the field stars around V404 Cygni. The color excess and PD showed a good correlation, and we estimated the color excess of V404 Cygni as $E(R_C - I_C) = 1.0 \pm 0.2$ and $E(B - V) = 1.2 \pm 0.3$, which corresponds to $A(V) = 3.7$ with $R_V = 3.1$. We also measured the upper limit of peak wavelength for multi-band PD as $\lambda_{\max} < 5500\text{\AA}$. It is known that a relation between λ_{\max} and R_V is described with the empirical formula $R_V = 5.5 \times 10^{-4} \lambda_{\max}$ (Serkowski et al. 1975). We obtained the upper limit of $R_V < 3.0$ and $A(V) < 3.6$ with $\lambda_{\max} < 5500\text{\AA}$. In addition, using another empirical relation of the maximum value of $P(V)/A(V) < 0.03 \text{ mag}^{-1}$ (e.g., Voshchinnikov & Das 2008), where $P(V)$ is the PD value at V-band, we obtained the lower limit of $3.0 < A(V)$. Finally, we obtained an extinction value of $3.0 < A(V) < 3.6$. This extinction value is consistent with the value of $2.2 < A(V) < 3.3$ reported in Shahbaz et al. (2003), but

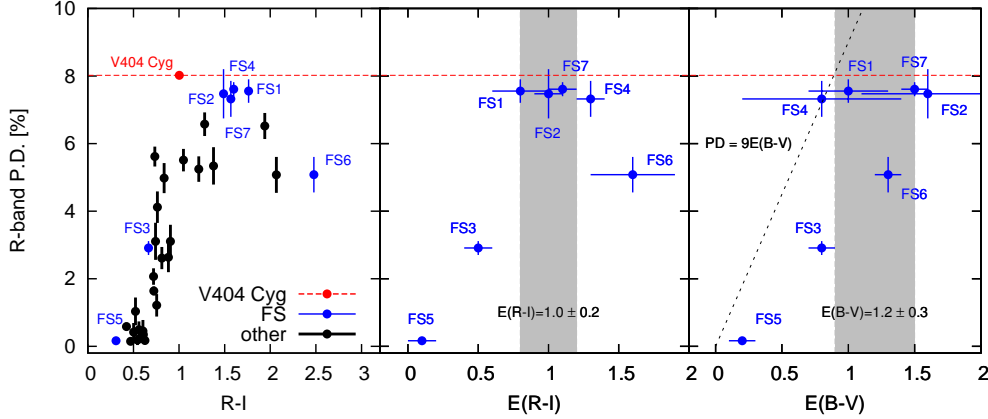


Fig. 5. Left panel shows scatter plot for polarization degree and color $R - I$, central panel shows scatter plot for polarization degree and estimated color excess $E(R - I)$ and right panel shows scatter plot for polarization degree and estimated color excess $E(B - V)$. Red data indicates the data of V404 Cygni, blue data indicate the data of Field stars (FS), and black data indicates the other field stars. In central and right panel, gray regions indicate the estimated $E(R - I)$ and $E(B - v)$ for V404 Cygni. Dashed line indicates the empirical maximum polarization degree as a function of $E(B - V)$ (Fosalba et al. 2002).

slightly low compared with the value of $A(V) = 4.0$ reported in Hynes et al. (2009). From X-ray observation, we also estimate the hydrogen column density via spectral fitting. Using relation between hydrogen column density N_H and $E(B - V)$ of $N_H = (6.86 \pm 0.27) \times 10^{21} E(B - V)$ (Güver & Özel 2009), $N_H = (8 \pm 2) \times 10^{21} \text{ cm}^{-2}$ is estimated with $E(B - V) = 1.2$ and this value is also consistent with X-ray observation of integrated hydrogen column density of $N_H = 6 - 12 \times 10^{21} \text{ cm}^{-2}$ during the outburst in 2015 (Radhika et al. 2016). In general, measurements of the Galactic extinction for X-ray binary systems are model-dependent (e.g., Shahbaz et al. 2003). On the other hand, our method does not include the uncertainties caused by the emission model of a comparison of stars and disks as it independent from the accurate intrinsic luminosity of binary systems. Our method is applicable to other Galactic transients that have no intrinsic polarization in the optical band.

The typical value of the interstellar PA within 3 degrees of V404 Cygni is about 35 ± 35 degrees (stellar polarization catalogs, Heiles 2000). Compared with this perspective trend of polarization in the Galactic plane, it is implied that local ISP around V404 Cygni is not irrelevant to the global Galactic ISP. On the other hand, the maximum PD of the ISP in the Galactic plane within 3 degrees for V404 Cygni is about $PD = 3.69 \pm 0.18$ for HD 331976 at $\lambda \sim 5400 \text{ \AA}$. Of course, this may be due to a lack of measurement of stellar polarization in this region (we have only 22 sources in the stellar polarization catalog within 3 degrees of V404 Cygni). However, the measured local ISP of $PD = 8.9 \pm 0.1\%$ for V404 Cygni in V -band and the color excess of $E(B - V) = 1.2$ are among the highest values in the Galaxy (Fosalba et al. 2002). The tendency of the bluer peak of polarization ($\lambda_{\text{max}} < 5500 \text{ \AA}$) suggested that the

dust grains toward the V404 Cygni region are generally smaller than the Galactic average.

Figure 6 shows the quasi-simultaneous spectral energy distribution (SED) of V404 Cygni, with a correction for Galactic extinctions with several $A(V)$ and R_V values. The SED data were taken by HONIR within 30 minutes on MJD 57194. For comparison, we showed the SED with $A(V) = 2.2 - 4.4$, $R_V = 3.1$, which are often used for correction for V404 Cygni, and the SED with no correction in Figure 6. There is a break between the J and I_C bands (corresponding to $2.5 \times 10^{14} \text{ Hz}$ and $3.7 \times 10^{14} \text{ Hz}$, respectively) for the SED with $A(V) = 3.0$, $R_V = 3.0$. In the optical band ($> 2.5 \times 10^{14} \text{ Hz}$), the SED with $A(V) = 3.0$, $R_V = 3.0$ shows a flat spectrum in the νF_ν regime. With the synchrotron emission model in the NIR and optical bands, this break indicates the break frequency due to synchrotron self absorption (SAA, defined as ν_{SAA}) which is an important value for estimating the magnetic field strength in the jet. The estimated ν_{SAA} value of $2.5 \times 10^{14} < \nu_{\text{SAA}} < 3.7 \times 10^{14} \text{ Hz}$ is consistent with the ν_{SAA} value assumed in Tanaka et al. (2016).

Acknowledgement

This work is supported by JSPS KAKENHI Grant Numbers 24000004. This work is also supported by JSPS and NSF under the JSPS-NSF Partnerships for International Research and Education (PIRE). This work is also supported by the Optical and Nearinfrared Astronomy Inter-University Cooperation Program by the Ministry of Education, Culture, Sports, Science and Technology of Japan. M.W. was supported by a Grant-in-Aid for Young Scientists (A) (25707007) from JSPS.

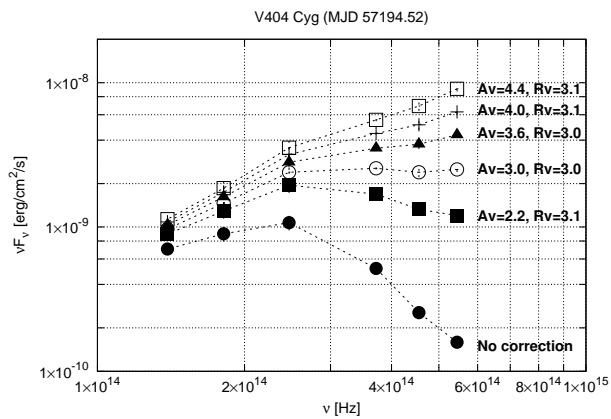


Fig. 6. Quasi-simultaneous spectral energy distribution (SED) of V404 Cygni on MJD 57194.52 with several correction of the Galactic extinction. Black filled circle data point indicates the SED without the Galactic extinction. Black box, open circle, black triangle, cross and open box data point corresponds to the SED with the Galactic extinction value of

$$A(V) = 2.2, R_V = 3.1, A(V) = 3.0, R_V = 3.0,$$

$$A(V) = 3.6, R_V = 3.0, A(V) = 4.0, R_V = 3.1 \text{ and}$$

$$A(V) = 4.4, R_V = 3.1 \text{ respectively.}$$

References

- Akitaya, H., et al. 2014, in Proc. SPIE, Vol. 9147, Ground-based and Airborne Instrumentation for Astronomy V, 914740
- Casares, J., Charles, P. A., Naylor, T., & Pavlenko, E. P. 1993, MNRAS, 265, 834
- Fosalba, P., Lazarian, A., Prunet, S., & Tauber, J. A. 2002, ApJ, 564, 762
- Güver, T., & Özel, F. 2009, MNRAS, 400, 2050
- Heiles, C. 2000, AJ, 119, 923
- Hynes, R. I., Bradley, C. K., Rupen, M., Gallo, E., Fender, R. P., Casares, J., & Zurita, C. 2009, MNRAS, 399, 2239
- Kawabata, K. S., et al. 2008, in Society of Photo-Optical Instrumentation Engineers (SPIE) Conference Series, Vol. 7014, Society of Photo-Optical Instrumentation Engineers (SPIE) Conference Series
- Kawabata, K. S., et al. 2014, ApJL, 795, L4
- Kimura, M., et al. 2016, Nature, 529, 54
- Lipunov, V. M., et al. 2016, ArXiv e-prints
- Miller-Jones, J. C. A., Jonker, P. G., Dhawan, V., Briskin, W., Rupen, M. P., Nelemans, G., & Gallo, E. 2009, ApJL, 706, L230
- Nagata, T. 1990, ApJL, 348, L13
- Poole, T. S., et al. 2008, MNRAS, 383, 627
- Radhika, D., Nandi, A., Agrawal, V. K., & Mandal, S. 2016, MNRAS, 462, 1834
- Schmidt, G. D., Elston, R., & Lupie, O. L. 1992, AJ, 104, 1563
- Serkowski, K., Mathewson, D. S., & Ford, V. L. 1975, ApJ, 196, 261
- Shahbaz, T., Dhillon, V. S., Marsh, T. R., Zurita, C., Haswell, C. A., Charles, P. A., Hynes, R. I., & Casares, J. 2003, MNRAS, 346, 1116
- Shahbaz, T., Fender, R. P., Watson, C. A., & O'Brien, K. 2008, ApJ, 672, 510
- Shahbaz, T., Ringwald, F. A., Bunn, J. C., Naylor, T., Charles, P. A., & Casares, J. 1994, MNRAS, 271, L10
- Shahbaz, T., Russell, D. M., Covino, S., Mooley, K., Fender, R. P., & Rumsey, C. 2016, MNRAS, 463, 1822
- Silva, D. R., & Cornell, M. E. 1992, ApJS, 81, 865
- Tanaka, Y. T., et al. 2016, ApJ, 823, 35

- Voshchinnikov, N. V., & Das, H. K. 2008, J. Quant. Spectrosc. Radiat. Transfer, 109, 1527
- Watanabe, M., Takahashi, Y., Sato, M., Watanabe, S., Fukuhara, T., Hamamoto, K., & Ozaki, A. 2012, in Proc. SPIE, Vol. 8446, Ground-based and Airborne Instrumentation for Astronomy IV, 844620
- Wenger, M., et al. 2000, A&AS, 143, 9
- Whittet, D. C. B., ed. 2003, Dust in the galactic environment
- Whittet, D. C. B., Martin, P. G., Hough, J. H., Rouse, M. F., Bailey, J. A., & Axon, D. J. 1992, ApJ, 386, 562